

# Employing Kinematic Uncertainty in EO Resolution Selection and Information-Theoretic Sensor Tasking

Richard E. Cagley, David E. Beckman, and Kevin J. Sullivan

Toyon Research Corporation, 75 Aero Camino, Suite A, Goleta, CA 93117

## ABSTRACT

The degree of uncertainty in a track's position provides an indication of how best to allocate sensor resources. In this paper, we discuss the use of this track parameter for two tasking activities. First, we consider determining resolution selection for electro-optical (EO) sensor tasks. Secondly, we integrate our knowledge of kinematics into the process of information-theoretic task selection. We consider the use of optimized selection of the resolution for imaging sensors such that we maximize what we term the probability of acquiring a target. The probability of acquiring, if a particular resolution is chosen, is a function of both the probability of the target being within the sensor footprint as well as the probability the target is detected given it is in the footprint. In the process of selection of sensor tasks, Toyon employs an information-theoretic metric. We apply conditionals on the entropy that are a function of the uncertainty with which the track will actually be detected during the sensor task. A tracker, based on the Kalman filter, is used to provide an estimate of position and an associated two dimensional error covariance. The kinematic information is used to compute the probability a target is within a footprint, whose size is based on the resolution. For simulation we employ the high fidelity Toyon-developed SLAMEM<sup>TM</sup> testbed.

**Keywords:** Electro-optical (EO), ladar, kinematics, sensor tasking, entropy

## 1. INTRODUCTION

Automated sensor management continues to draw increasing levels of interest through both research and system development. While previously it may have been possible for a pilot or aircraft operator to task and collect data from on-board sensors, the expanding number of sensors and the raw amount of data make this task daunting for even the most capable individuals. Thus, the operator is often relieved to relinquish this control in order to obtain higher level knowledge, such as threat warnings or automated search of a region of interest. However, the problem of sensor task creation and ordering its execution is complex, with many techniques available.<sup>1</sup> Figure 1 shows a high-level overview of a typical Intelligence, Surveillance, and Reconnaissance (ISR) architecture. Here, multiple stand-off assets, whether manned or unmanned, possess one or more sensors that can be tasked with different parameters, such as resolution or direction. In this paper, we discuss the role uncertainty in a target's location can play in both sensor task creation as well as schedule creation. In particular, we consider electro-optical (EO) sensors with variable resolutions and propose a method whereby an optimum resolution can be selected. Secondly, we consider an enhancement to Toyon's information-theoretic approach to schedule evaluation in which the certainty of a target's location is integrated. In addition to analysis, we present simulations that indicate possible gains in performance.

## 2. EO TASK CREATION

Certain imaging sensors have the ability to vary their resolution. Thus, aboard many unmanned aerial vehicles (UAVs) the operating resolution can be selected during task creation.<sup>2</sup> Typically, an operator will initially choose a large image footprint and then zoom in when a target of interest is discovered. Conceptually, we seek to provide a similar automated approach based on some metric of performance that decides what an optimum resolution would be for imaging a particular track. The role of EO task creation, and the associated algorithm for performing dynamic resolution selection (DRS) is shown in Figure 2. The process consists of looping through

---

Further author information  
E-mail: rcagley@toyon.com

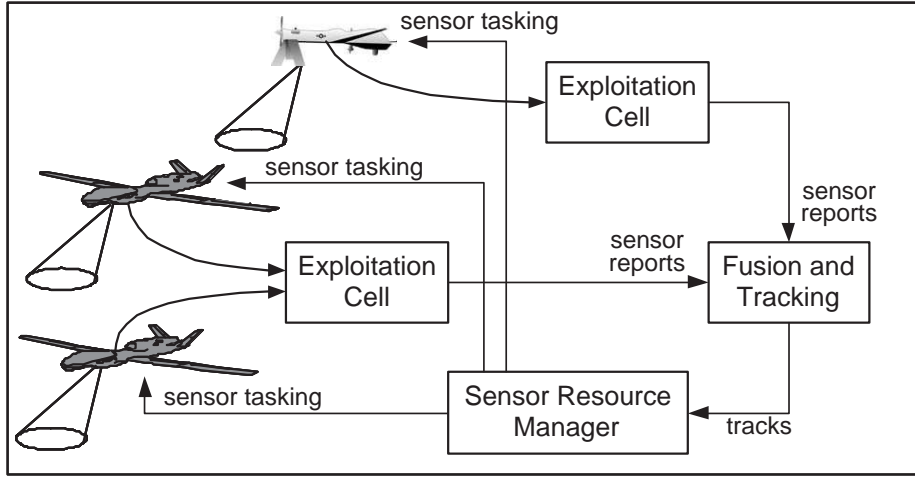


Figure 1. ISR Architecture.

all possible tracks, determining whether an EO sensor can be used, and then finally selecting the resolution that would yield the best performance for that track.

Intuitively, there will be an optimal resolution such that the probability of obtaining sensor information on the target is maximized. We will refer to this event as acquiring the target. Thus, when a sensor image is placed, the two possibilities  $\{A, \tilde{A}\}$  denote the set whereby the target is either acquired or not. The probability of acquiring the target can be written as

$$P(A) = P(A|F)P(F) + P(A|\tilde{F})P(\tilde{F}) \quad (1)$$

where  $F$  and  $\tilde{F}$  denote whether or not the target is located within the sensor footprint. The second term  $P(A|\tilde{F}) \equiv 0$  is due to the fact that if the target is not located within the sensor footprint then it cannot be acquired. The term  $P(A|F)$  will increase as the resolution becomes finer. This is due to the fact that with finer resolution, it is more likely the sensor can discern the target from other objects and ground clutter. The second term,  $P(F)$ , is inversely proportional to the fineness of the resolution; with finer resolution the sensor footprint size will decrease making it less likely the target is within the footprint. We see the two terms that generate  $P(A)$  are inversely dependent on resolution. Intuitively, we expect there to be a particular resolution that maximizes  $P(A)$ .

To simplify notation, we let  $P_D \triangleq P(A|F)$ . The term  $P_D$  denotes the probability the sensor is able to detect the target given that it is within the sensor footprint. These terms are generated by Johnson's criteria.<sup>3</sup> According to this criteria, the probability of detection ( $P_D$ ) can be computed with the equation

$$P_D = \frac{r^E}{1 + r^E} \quad (2)$$

where  $E \triangleq 2.7 + .7r$  and  $r$  is computed as  $r \triangleq N/N_{50}$ . For this equation,  $N$  is the number of resolvable cycles across the target and  $N_{50}$  is the line pair criteria, which for our purposes will be detection performance. The  $N_{50}$  values were derived from field tests. We compute  $P_D$  as a function of resolution and target type. Because there are different probabilities associated with a track being of particular target types, and associated  $P_D$ s, we choose the  $P_D$  associated with the most likely target type.

Additionally, we define the expectation that the target will be in the footprint as  $P_I \triangleq P(F)$ . This value can be computed by integrating the probability density, corresponding to the target position, over the region inside the sensor footprint. Unfortunately, integrating in this manner will not lead to a solution that is straightforward to compute. Thus, we seek an approximation that yields a more manageable form. Our method is depicted in Figure 3 and discussed in the next section.

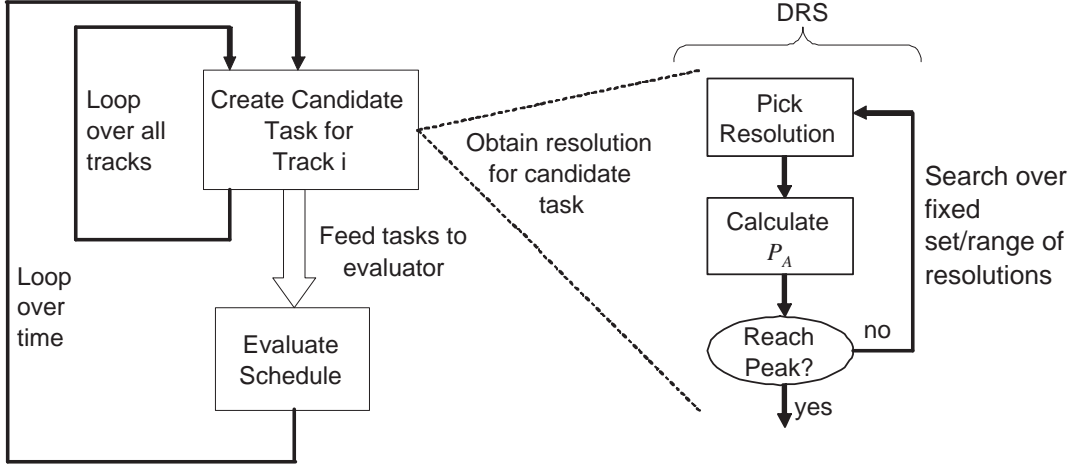


Figure 2. Location of DRS within sensor tasking architecture.

### 2.1. Finding an Approximation for $P_I$

Here, we provide a method for determining the probability the TOI lies within the EO spot. Because we have a model for the position uncertainty,  $P_I$  can be found by simply integrating over the probability density function corresponding to the position of the target. Our model is a joint Gaussian density given by

$$f_{X,Y}(x,y) = \frac{1}{2\pi\sigma_X\sigma_Y\sqrt{1-\rho^2}} \exp\left(\frac{-1}{2(1-\rho^2)} \left\{ \left(\frac{x-\mu_X}{\sigma_X}\right)^2 - 2\rho\left(\frac{x-\mu_X}{\sigma_X}\right)\left(\frac{y-\mu_Y}{\sigma_Y}\right) + \left(\frac{y-\mu_Y}{\sigma_Y}\right)^2 \right\}\right) \quad (3)$$

where  $\mu_X$  and  $\mu_Y$  are the means of the  $x$  and  $y$  target positions.<sup>4</sup> Similarly,  $\sigma_X^2$  and  $\sigma_Y^2$  are the associated variances and  $\rho$  is the cross-correlation.<sup>4</sup>

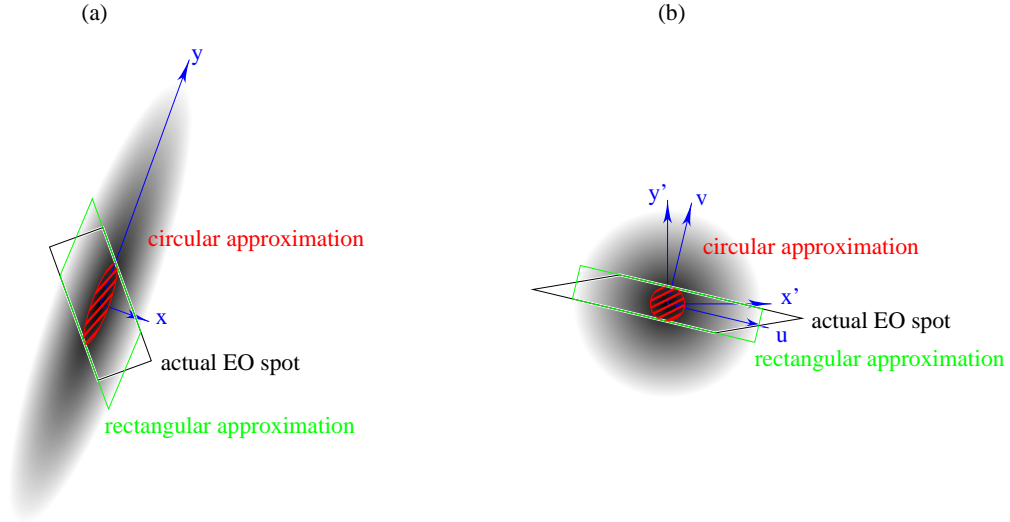


Figure 3. EO footprint and position error covariance: (a) ground coordinates (b) transformed coordinates.

In order to decouple the coordinate positions, thereby easing integration, we use a transformation matrix. This begins by obtaining an eigendecomposition of the covariance matrix which is given by  $\Sigma = \mathbf{U}\mathbf{D}\mathbf{U}^T$ . Here, the matrix  $\mathbf{U} = [\mathbf{u}_1 \mathbf{u}_2]$  holds the eigenvectors and the diagonal matrix  $\mathbf{D} = \begin{bmatrix} \lambda_1 & 0 \\ 0 & \lambda_2 \end{bmatrix}$  holds the corresponding

eigenvalues. The resulting transformation matrix  $\mathbf{C} = (\mathbf{U}\sqrt{\mathbf{D}})^{-1}$  rotates and scales the covariance matrix of our joint Gaussian such that it becomes an identity matrix. An example EO spot once the transformation matrix  $\mathbf{C}$  has been applied is shown in Figure 3.

Once the new coordinate system has been constructed, we find an approximation of the density over the resulting footprint. In our new coordinate space, we note the axis variables are now given by

$$\begin{bmatrix} x' \\ y' \end{bmatrix} = \mathbf{C} \begin{bmatrix} x \\ y \end{bmatrix}. \quad (4)$$

with the resulting probability density

$$f_{X',Y'}(x',y') = \frac{1}{2\pi} \exp\left(-\frac{1}{2}(x'^2 + y'^2)\right). \quad (5)$$

As can be seen in Figure 3, our approximate area consists of a rectangle formed by the longer side of the transformed spot along with a line perpendicular to this longer side, centered midway through the short side. Noting that the resultant probability density is isotropic, we can integrate over the EO spot along the  $u$  and  $v$  axes shown in Figure 3. That is, for the approximate EO spot area  $Z$  we have

$$\begin{aligned} P_I &= \iint_Z f_{X',Y'}(x',y') dx' dy' \\ &= \frac{1}{2\pi} \int_{-L/2}^{L/2} \int_{-S/2}^{S/2} \exp\left(-\frac{1}{2}(u^2 + v^2)\right) du dv \\ &= \operatorname{erf}\left(\frac{L}{2\sqrt{2}}\right) \operatorname{erf}\left(\frac{S}{2\sqrt{2}}\right) \end{aligned} \quad (6)$$

where  $L$  and  $S$  are the side lengths for the approximate EO spot and erf is the error function.<sup>4</sup>

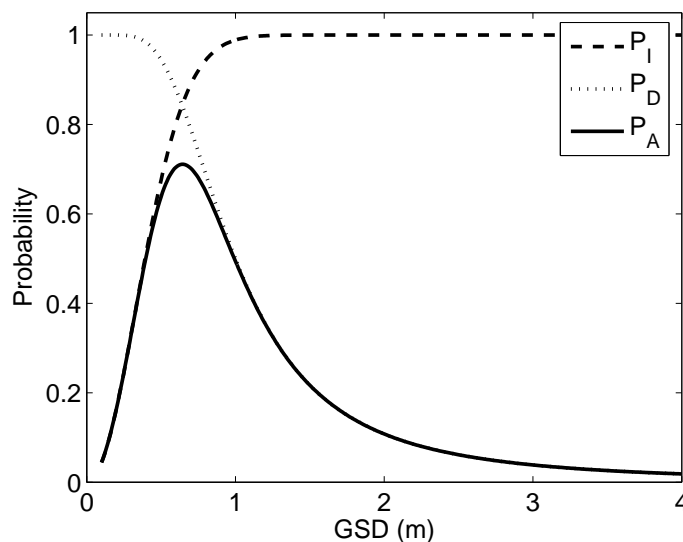


Figure 4. Probabilities as a function of resolution.

## 2.2. Searching for Optimal Resolution

The process of choosing the best resolution requires searching through the possible values and computing  $P_A$  for each. Thus, the resolution that maximizes  $P_A$  is selected for the candidate task. Here, we consider an EO

sensor that has a finite set of resolutions, denoted by ground sample distance (GSD). In this case, the algorithm can simply select the GSD that maximizes the probability of acquiring the target. To lend an intuitive feel for the tradeoff between  $P_D$  and  $P_I$  which provide the resulting value for  $P_A$ , example values are plotted for a range of GSDs in Figure 4. For this example,  $P_D$  is computed with  $r \equiv 1/\text{GSD}$  and the footprint width is  $L = S = 3/\text{GSD}$ . As can be seen from the figure, there is a maximum value for  $P_A$  over the range of GSD values.

### 3. USING TRACK LOSS PROBABILITY IN TASK SELECTION

Toyon employs an information-theoretic approach to sensor schedule evaluation.<sup>5,6</sup> Thus, we seek to reduce the total level of uncertainty in track identification.<sup>7</sup> Using Shannon’s information theory, entropy for the random variable, track identification, is given by

$$H(p) = - \sum_{n=1}^N p_n \log(p_n) \quad (7)$$

where  $p_n$  is the probability that the target belongs to the  $n$ th of  $N$  target types.<sup>8</sup> Information theory for sensor tasking relies on the ability to compute expected entropy. We then select the sensor schedule that minimizes the total expected entropy for all tracks.<sup>9</sup> Through experimentation, we have discovered cases in which an approach based purely on track identification can lead to undesirable results. Consider the case in which several targets of interest (TOIs) have been classified with a high degree of certainty. This scenario is quite common as an EO sensor has the ability to offer excellent identification performance. In this scenario, the schedule evaluator will not retask a sensor on these TOIs unless they become confused with another track resulting in loss of classification. However, such events may take several minutes to occur. Thus, because track location uncertainty can increase quickly, leading to a lost TOI, our motivation is to retask on a well classified target if we have degraded knowledge of its kinematic state. Approaches to combined information and kinematic tasking have been proposed<sup>10</sup>; here, we seek a computationally tractable solution.

The general idea is to task sensors to targets that have a large position covariance. The reasoning is that the next sensor revisit to acquire the target may be unsuccessful since knowledge of the target’s position may be so poor that the target will not be inside the sensor footprint. By keeping the covariance small through frequent updates of the target’s position, we are better able to keep it in track. The location of the algorithm within the overall sensor tasking architecture is shown in Figure 5. As seen in the figure, track loss probability (TLP) is used in evaluating the score of a schedule. Some of the difficulties with incorporating TLP into our cost function include:

1. Our tracker extrapolates the track to multiple states (a road split is one example). Some of these will have a higher probability of being the target location than others. A problem arises when states with low probability are tasked due to their high levels of kinematic uncertainty.
2. While the cost typically weights more heavily towards TOIs than civilians, our new cost may attempt to go after civilian targets with poor position information.
3. The cost function currently weights acquiring ambiguous tracks more heavily through an averaging of entropies. With our modified cost, we could potentially weight tracks with poor position knowledge over ambiguous tracks.

As will be seen in Section 4, these issues limit the performance of schedule evaluation with TLP. The inclusion of other techniques, such as DRS, can overcome certain deficiencies.

Before we present the modified expression for entropy, we define the following terms:

- A: Represents acquiring the target. That is, if we put down a footprint the target is recognized by the sensor. Typically, this will involve the target being both inside the footprint and being detected by the sensor. However, here we leave the term general.

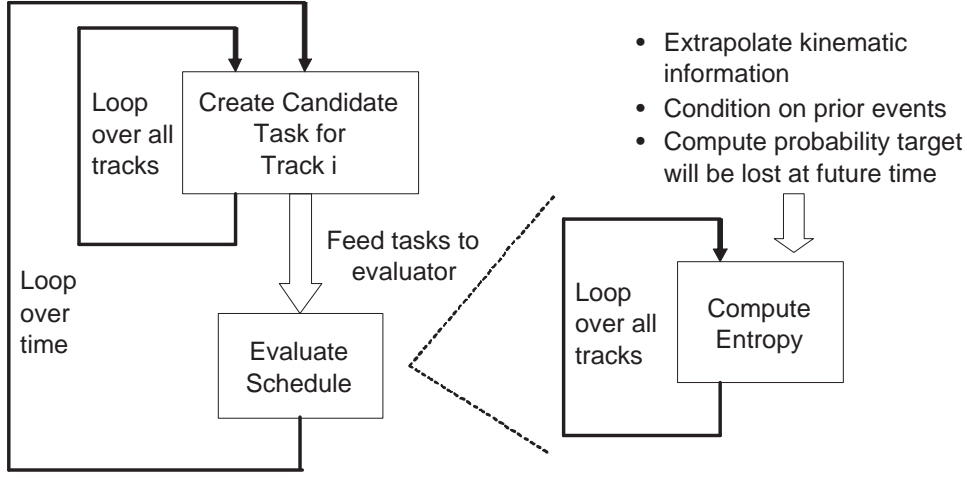


**Figure 5.** Role of Kinematics within sensor tasking architecture.

- $L$ : This term refers to target loss at the end of the evaluation time horizon for sensor schedule evaluation. That is, if we were to revisit the target with a standard size footprint, would we acquire the target? If not, then we say that it is likely the target will not be detected again and hence the track will be lost.

Using total probability, we expand the entropy as

$$H = (H|A)P(A) + (H|\tilde{A})P(\tilde{A}) \quad (8)$$

where  $P(\tilde{A})$  can also be written as  $1 - P(A)$ . The conditional entropy expressions can be expanded as

$$\begin{aligned} (H|A) &= (H|A, \tilde{L})P(\tilde{L}|A) + (H|A, L)P(L|A) \\ &= \hat{H}P(\tilde{L}|A) + H_{\text{Max}}P(L|A) \end{aligned} \quad (9)$$

and

$$\begin{aligned} (H|\tilde{A}) &= (H|\tilde{A}, \tilde{L})P(\tilde{L}|\tilde{A}) + (H|\tilde{A}, L)P(L|\tilde{A}) \\ &= H_{\text{Old}}P(\tilde{L}|\tilde{A}) + H_{\text{Max}}P(L|\tilde{A}) \end{aligned} \quad (10)$$

where we have let  $\hat{H}$  denote the updated entropy assuming that the target is acquired (and hence gets an update via a sensor measurement) and that it will not be lost at the end of the task evaluation time. For our second equation, the term  $H_{\text{Old}}$  denotes the case in which the target classification has not been updated via a sensor measurement, but will not be lost due to poor position knowledge. For the last entropy term, if the target is lost then we assume that the entropy will be maximized providing a high cost for losing a target. This value is given by

$$H_{\text{Max}} = \log(N) \quad (11)$$

where we have assumed that in the maximum entropy case all  $N$  types of targets are equally likely. Finally, we note that we can make the approximation

$$(H|A) \simeq \hat{H} \quad (12)$$

if we assume that the probability of losing a track is approximately zero if the track was acquired. That is, through a sensor measurement we are able to provide sufficient accuracy in the position measurement such that the target is not lost.

Now that we have discussed the entropy expressions, we can look at the expressions for the probability of losing a track conditioned on the event that the target was not acquired. This term can be expanded as

$$P(L|\tilde{A}) = \sum_{l=1}^L P(L|\tilde{A}, s_l)P(s_l|\tilde{A}) \quad (13)$$

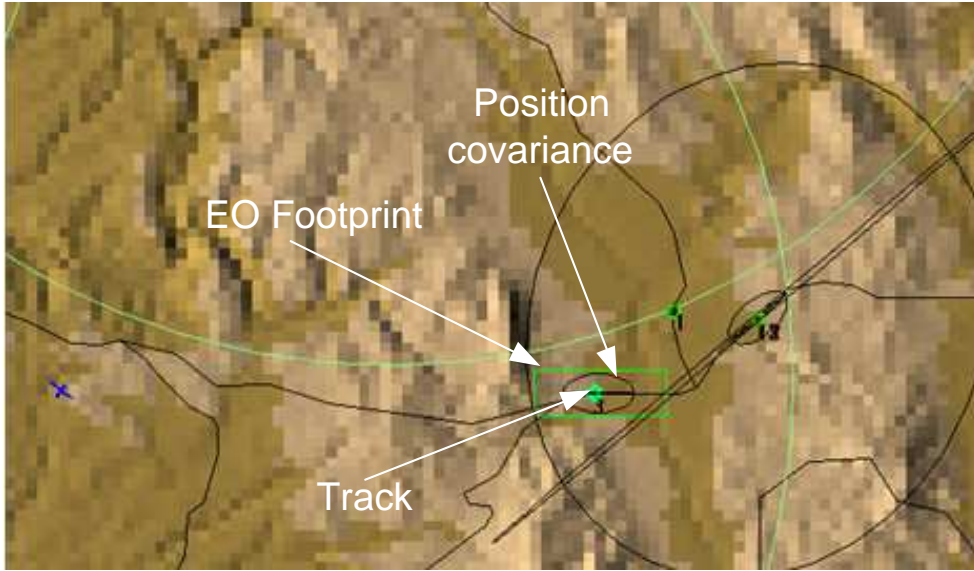


**Figure 6.** Snapshot of SLAMEM testbed running simulated case.

where  $s_l$  denotes extrapolated state  $l$  of the  $L$  states for the current target under consideration. The probabilities of these states ( $P(s_l)$ ) are given by the tracker along with their associated covariance matrices. To estimate the probability of loss, we will compute the integral of the density over a circle of radius  $\gamma$ . Letting  $\sigma^2 \equiv \sqrt{\det(C_l)}$  be an estimate of the position covariance, where  $C_l$  is the covariance for state  $l$ , we can obtain an expression for the density of the state position:

$$f_{x,y} = \frac{1}{2\pi\sigma^2} \exp\left(-\frac{1}{2} \frac{x^2 + y^2}{\sigma^2}\right). \quad (14)$$

Note that we have constrained the density such that the  $x$  and  $y$  positions have equal covariance and are uncorrelated to ease in computation of the integral to follow. Using a change of variables into polar coordinates, an expression for the probability of loss can be written as

$$\begin{aligned} P(L|\tilde{A}, s_l) &= 1 - \frac{1}{2\pi\sigma^2} \int_0^{2\pi} \int_0^\gamma \exp\left(-\frac{1}{2} \frac{r^2}{\sigma^2}\right) r \, dr \, d\theta \\ &= \exp\left(-\frac{1}{2} \frac{\gamma^2}{\sigma^2}\right). \end{aligned} \quad (15)$$

Note the footprint size  $\gamma$  can be chosen to meet different goals. Here, we use the maximum candidate EO sensor footprint size in order to avoid track loss upon EO retasking. An alternative would be to specify a fixed size for cases such as targeting.

#### 4. COMPUTER SIMULATIONS

For analysis of our enhancements to sensor task creation and schedule evaluation, we used the Toyon-developed simulation testbed SLAMEM<sup>TM</sup> (Simulation of the Location and Attack of Mobile Enemy Missiles). SLAMEM makes an excellent testbed for the development and testing of ISR algorithms as it contains models of the relevant components of the ISR environment such as terrain elevation data, road networks, and foliage. Figure 6 provides a screenshot of the simulation where vehicles, the road network, as well as stand-off aircraft and their associated field of views (FOVs) are shown. SLAMEM contains a detailed ground-vehicle-motion model that takes into consideration vehicle interactions, right-of-way logic at intersections, and variable vehicle speeds. Sensor platforms such as satellites, aircraft, and ground vehicles are modeled. Sensors such as GMTI, SAR, and EO are modeled to the level of detail necessary to account for an accurate representation of where and when

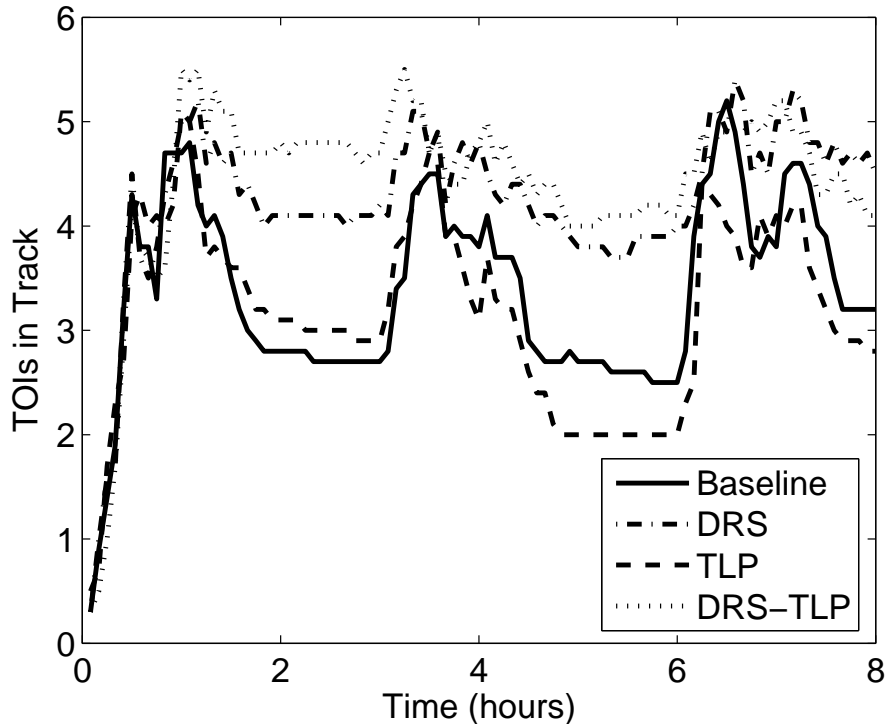


**Figure 7.** Monte Carlo simulation with different combinations of tasking enhancements.

they image a portion of the ground. Models and algorithms for tasking, fusion, and exploitation are contained within SLAMEM. In particular, we use an interacting multiple model (IMM) tracker.<sup>11</sup>

For our simulation, we considered an environment with six TOIs and 40 civilian confusers. There are four Predator UAVs statically tasked to fly in a triangular pattern, where they are evenly separated in distance. In addition, two GlobalHawks provide stand-off radar coverage with both high-resolution radar (HRR) as well as moving-target identification (MTI) radar. The test case presents a challenging scenario with such features as road splits, stop-move-stop, and obscurations. During simulation, we considered all combinations of both DRS and TLP being both on and off. Ten Monte Carlo runs, each with a simulated time of eight hours, were run and the results for the four cases are shown in Figure 7. From the figure, it is clear DRS offers performance gains in all cases. The same cannot be said with the inclusion of TLP. With only TLP added, there is a period of performance gain and another period with worse performance. The major cause of this mixed performance is that TLP will weight extrapolated states with high kinematic uncertainty even though they may have low probability of being associated with the track. However, if DRS is included, larger footprints often allow multiple extrapolated states to be imaged simultaneously overcoming the deficiency. Thus, when both DRS and TLP are used we see the highest level of performance.

## 5. CONCLUSION

The area of sensor management is rapidly developing due to the increasing demands placed on the operators of airborne assets. In this paper we addressed the practical inclusion of kinematic information in two specific areas of an overall sensor management architecture. In terms of sensor task creation, we provided a DRS algorithm that is able to select an EO imager parameter, the resolution, that is optimized in terms of keeping a TOI in track. Similarly, for schedule evaluation, we proposed a technique whereby TLP can be integrated into an information-theoretic based valuation of a schedule. Through simulation, on the Toyon-developed SLAMEM testbed, we evaluated the performance of each algorithm individually as well as when both techniques were

applied to sensor management. We demonstrated the ability to significantly increase the number of TOIs that were able to be continuously maintained in track over the lifetime of the simulation.

## ACKNOWLEDGMENTS

The work presented here was supported under contract No: F33615-03-C-1454 by Air Force Research Labs (AFRL). The authors would like to thank Mark R. Meloon and Kevin H. Andrew for their assistance with simulation.

## REFERENCES

1. S. Musick and R. Malhotra, "Chasing the elusive sensor manager," in *Proc. of IEEE 1994 National Aerospace and Electronics Conference*, pp. 606–613, 1994.
2. J. M. Borky, "Payload technologies and applications for uninhabited air vehicles (UAVs)," in *Proc. of the IEEE Aerospace Conference*, **3**, pp. 267–283, Feb. 1997.
3. J. Johnson, "Analysis of image forming systems," in *Proc. of the Image Intensifier Symposium*, pp. 249–273, Oct. 1958.
4. P. Z. Peebles, *Probability, Random Variables, and Random Signal Principles*, McGraw Hill, New York, 1993.
5. N. Xiong and P. Svensson, "Multi-sensor management for information fusion: issues and approaches," *Information Fusion* **3**, pp. 163–186, 2002.
6. K. Sullivan, C. Agate, and H. Berger, "Allocation of radar resources to maximize tracker information," in *Proc. 14th National Symposium on Sensor Fusion*, August 2001.
7. W. Schmaedeke, "Information based sensor management," in *Proc. SPIE Conference on Target Recognition and Data Fusion II*, May 1993.
8. C. Shannon, "A mathematical theory of communication," *Bell System Technical Journal* **27**, pp. 379–423, July 1948.
9. K. J. Hintz, "A measure of the information gain attributable to cueing," *IEEE Trans. on Systems, Man, and Cybernetics* **21**, pp. 237–244, March 1991.
10. G. A. McIntyre, *A Comprehensive Approach to Sensor Management and Scheduling*. PhD thesis, George Mason University, 1998.
11. X. R. Li, "Engineer's guide to variable-structure multiple-model estimation for tracking," in *Multitarget-Multisensor Tracking*, Y. Bar-Shalom and W. D. Blair, eds., ch. 10, Artech House, 2000.